A Quasiclassical Trajectory Study of the Multichannel H(1) + H(2)BO → BO + H_2, H(1)BO + H(2), HOB + H Reaction

M. Albertí,* J. M. Lucas, and A. Aguilar

Departament de Química Física i Centre de Recerca en Química Teòrica, Universitat de Barcelona, C/ Martí i Franquès, 1. 08028 Barcelona, Spain

Received: May 24, 2002; In Final Form: October 10, 2002

The dynamics of the multichannel H(1) + H(2)BO → BO + H_2, H(1)BO + H(2), HOB + H reaction has been studied by quasiclassical trajectory calculations on an analytical potential energy surface, which was previously used to analyze the dynamics of the BO + H_2 reaction. The results reported here include integral and differential cross-sections, product angular distributions, and energy disposal for the H(2)BO molecule in the vibrational ground state (0,0,0) at 300 K of rotational temperature. Considering BH and BO stretching and bending excitations as well as several rotational temperatures, the influence of vibrational and rotational energies on reactivity was also analyzed. For the title reaction, three channels are open at the highest energies considered. There is a sharp increase in the reaction cross-section yielding H(1)BO + H(2) with the translational energy once this product channel becomes open. The overall reactivity depends on the initial energy type. Results for the forward H + HBO reaction are discussed and, when possible, compared with those for the BO + H_2 reverse reaction.

1. Introduction

The detailed dynamic study of chemical reactions involving more than three atoms is a field of considerable interest.[1−12] In recent years, thanks to continuous improvements in methodological, computational, and experimental fields, it has become possible to analyze several aspects of the reaction dynamics that are not present in triatomic systems. For instance, neither the different behavior of reactive and nonreactive bonds when reactant vibrational excitation is taken into account nor the selectivity of energy requirements can be studied in triatomic reactions. In terms of bimolecular reactions, the simplest situation in which such effects can be observed is for those reactions involving four atoms, i.e., diatom−diatom and atom−triatom reactions. The study of these dynamic aspects becomes particularly interesting when results for both forward, ABC + D → AB + CD, and reverse, AB + CD → ABC + D, reactions can be compared, as is evident from the studies of H + HCN → CN + H_2 and CN + H_2 → H + HCN reactions.[13−21] Several experiments on the H_2 + CN reaction and its isotopic variants were carried out, analyzing the role of the CN bond[13,14] as well as the angular and product translational energy distributions.[15] Experimental results were compared with those obtained from theoretical calculations, in which the role of the nonreactive CN bond was also investigated.[16−19] For the H + HCN → CN + H_2 reaction, in which HCN is vibrationally excited, the experimental CN state distributions were obtained.[4] These distributions showed a significant vibrational excitation of the CN product, thus indicating that the CN bond participates in the dynamics of the reaction. On the other hand, the influence of rotation and vibration on the reactivity and the dynamics of X + HCN (ν_1, ν_2, ν_3, j) (with X = H, Cl) were also studied.[20] Troya et al.[21] in a quasiclassical trajectory study (QCT) of the H + HCN reaction found that the vibrational excitation affected the reactivity.

Here, we study the dynamics of the H + HBO reaction, which is isoelectronic with H + HCN. Among other aspects, we analyze the effect of the reactant energy upon partial reactive cross-sections, the reaction mode, the product's angular distribution, and the product's energy disposal.

Several efforts have been made to understand both the kinetics and the dynamics of the reverse BO + H_2 → H + HBO reaction. For instance, conventional transition state theory calculations with a tunneling correction through an Eckart barrier show a curvature in the Arrhenius plot for the rate constant over a wide temperature range.[22] The author attributed this curvature at low temperatures to the tunneling effect. At higher temperatures, it was explained in terms of the temperature dependence of the vibrational partition function, which arises from the anomalously low doubly degenerate bending frequencies at the saddle point. Experimental rate constants as a function of the temperature (in the 690−1030 K range) were measured, and the results were compared with transition state theory calculations using a new scaled frequency of the doubly degenerate bend of the HHBO transition state in analogy with the isoelectronic HHCN transition state and lowering the calculated barrier by 1 kcal/mol.[23]

The dynamics of the BO + H_2 reaction was also investigated.[24−26] QCT calculations were performed using a six-dimensional potential energy surface (PES) constructed on the basis of experimental evidences.[24] In particular, analysis of the sensitivity of the reaction rate to reactant vibrational excitation showed that the vibrational excitation on the H_2 increases reactivity, while the excitation of BO inhibits the reaction. Results were interpreted in terms of the characteristics of the transition state normal mode(s) correlating with the corresponding asymptotic states. To analyze the role of the BO bond, QCT calculations considering several hypothetical isotopes of the BO molecule were run,[25] for selected rovibrational levels of the reactants, on the same PES at low and moderate collision energies. For all of these hypothetical systems, the selectivity of the reactant vibrational energy was studied in detail. Recently,

* To whom correspondence should be addressed. E-mail: maw@qf.ub.es.

10.1021/jp026173n CCC: $25.00
Published on Web 01/23/2003

a reduced dimensionality quantum mechanical study of the reaction showed a large contribution of tunneling effect to the reactivity in the threshold energy region.[26]

While several authors have studied both the kinetics and the dynamics of the BO + H_2 → H + HBO reaction, little is known about the H + HBO multichannel reaction, [27] which is particularly interesting because three product channels can be open

$$\mathrm{H(1) + (2)HBO} \rightarrow \mathrm{BO + H_2} \quad \Delta H_{298K}^{\circ} = 37.11 \text{ kJ mol}^{-1}$$

$$\rightarrow \mathrm{H(1)BO + H(2)} \quad \Delta H_{298K}^{\circ} = 0 \text{ kJ mol}^{-1}$$

$$\rightarrow \mathrm{HOB + H} \quad \Delta H_{298K}^{\circ} = 199.58 \text{ kJ mol}^{-1}$$

Nevertheless, both forward and reverse reactions are important not only to learn about the boron oxidation and the efficient use of boron-based materials as a rocket fuel[27] but also in theoretical chemistry studies such as the isoelectronic H + HCN → CN + H_2 and CN + H_2 → H + HCN reactions. Moreover, the fact that different reaction products can be formed adds interest to this study.

Here, the H + HBO reaction has been investigated by performing extended full-dimensional QCT calculations on the analytical PES, reported previously.[24] Several studies have shown that QCT results are often quantitative even at the state-resolved level.[28,29] Furthermore, QCT calculations have been proved to be very useful to analyze the dynamics of four center reactions.[30−36]

The present work, as mentioned above, is mainly oriented toward studying the reactivity and the reaction mechanism at several collision energies and the details of how reactant excitation in a specific mode can modify that mechanism, thus influencing both the reactivity for each channel and the energy partitioning in the products. Hence, a large range of collision energies covering several vibrational reactant states and different rotational temperatures was considered. Results will be compared, when possible, with those for the BO + H_2 → HBO + H reaction, thus completing the study of the role of the BO bond that was previously carried out for the reverse reaction.[24]

2. PES and Computational Details

QCTs have been run in the same six-dimensional PES used to study the dynamics of the BO + H_2 reaction.[24−26] Because this surface has been presented in detail elsewhere,[24] we here limit ourselves to a brief description of its most relevant features. The analytical PES was constructed following the Sorbie−Murrell method[37] that has previously been successfully applied to describe many other systems.[27,37] The method consists of expanding the overall potential as a sum of mono-, bi-, tri-, and tetratomic terms. In particular, the potential describing the interaction of the HHBO system, among all possible triatomic terms, only includes the HBO term. The H_2O and BH_2 triatomic terms were not included because they lie well above the energies used in the present study (H_2O and BH_2 are situated about 340 and 520 kJ mol^{-1}, respectively, above the reactants).[27] To describe the interaction potential as well as possible, a sum of two four body terms was considered.

The analytical PES shows a linear transition state (TS1) located at 73.01 kJ mol^{-1} above reactants, connecting them with BO + H_2 products. Unlike what was found for the reverse reaction, with only one accessible product channel, here, the products H(1)BO + H(2) (hydrogen atom exchange) and HOB + H (both H(1)OB and H(2)OB) are also accessible from reactants surmounting high-energy barriers. Figure 1 shows a schematic representation of the HBO + H reaction energy profile.

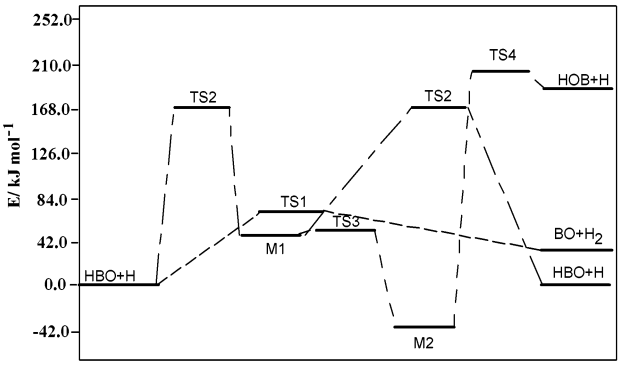

Figure 1. Schematic energy profile on the analytical PES, where the energies are referred to the reactants energy.

As can be seen, two minima are characterized, M1 (54.06 kJ mol^{-1} above reactants), with C_{2v} symmetry, and M2 (31.34 kJ mol^{-1} below reactants), which shows trans geometry (C_s symmetry). Both minima are connected through an isomerization barrier whose transition state (TS3) is located at 5.31 kJ mol^{-1} above the M1 minimum. From this profile, it seems evident that changes in the reaction mode can be observed going from low and moderate collision energies to the highest ones. The H(1)BO + H(2) products can be reached from H(1) + H(2)BO reactants surmounting a barrier of about 174 kJ mol^{-1} through the linear TS2 transition state, which connects reactants with the M1 minimum. Moreover, the HOB + H products can be formed when the collision energy is high enough to reach the nonlinear TS4 transition state, located at 233 kJ mol^{-1} above the M2 minimum. Thus, at high collision energies, both H(1)-BO + H(2) and HOB + H products should be obtained in addition to the BO + H_2 ones.

Classical trajectories were run on the above PES using an improved version (POLQCT[38]) of Hase's MERCURY computer program.[39] Hamilton's equations of motion were numerically integrated by combining the fourth-order Runge−Kutta and sixth-order Adams−Moulton algorithms. The integration step was chosen to be 6.25×10^{-17} s; this number is small enough to ensure the energy and momentum conservation with a difference lower than 0.01%. The fixed initial conditions are the vibrational energy of each HBO normal mode, the rotational temperature, the relative translational energy, the maximum impact parameter, and the initial distance between the reactant's centers of mass. From a given rotational temperature, any given reactant's rotational energy is selected. As indicated previously,[27] the selection method gives an averaged rotational energy, leading to the value $(3/2)k_BT$ for a large enough sampling. The remaining initial conditions were selected randomly following, as usual, the Monte Carlo method.[40] Trajectories were started at the distance of 12 Å between the H atom and the HBO center of mass; the interaction energy was negligible at this distance. The maximum impact parameter was determined separately for every set of initial conditions.

The reaction of translationally hot H atoms with HBO molecules in its ground vibrational state at 300 K of rotational temperature was studied at 10 translational energies in the 75.0−226.0 kJ mol^{-1} range, running sets of 1 500 000 trajectories at each initial condition, except at the lowest energy, where it was necessary to calculate 2 000 000 trajectories to obtain reactive cross-sections with statistical errors lower than 10%.

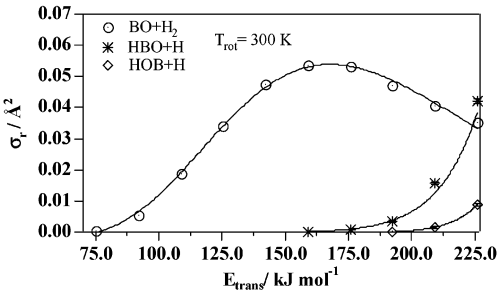

Figure 2. Reaction cross-sections vs translational energy for the H + HBO (0,0,0) reaction for the different reaction channels.

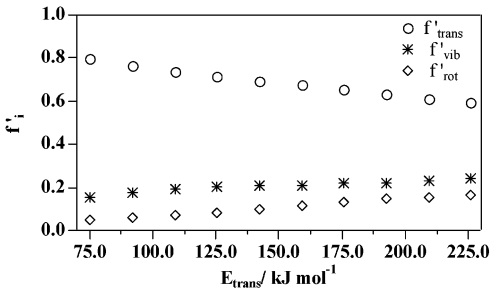

Figure 3. Energy distribution for the BO + H_2 products in terms of the fraction of accessible energy at different translational energies (reactant HBO in its ground vibrational state and T_{rot} = 300 K).

The influence of vibrational excitation on a specific mode was analyzed at 75.31 kJ mol^{-1} of translational energy and at 300 K of rotational temperature. Specific comparisons were also made at other translational energies. Finally, the influence of the reactant rotation was studied, mainly at 175.73 kJ mol^{-1} of translational energy; the HBO molecule was in its ground vibrational state. These studies were performed by running sets of at least 500 000 trajectories at each initial condition.

More than 25 000 000 trajectories were calculated to study the HBO + H reaction dynamics in the energy range considered, and five different rearrangement channels have been considered as follows: (i) H(2)BO + H(1) (reactants), (ii) BO + H_2, (iii) H(1)BO + H(2), (iv) H(2)OB + H(1), and (v) H(1)OB + H(2).

3. H + HBO (0,0,0; T_{rot} = 300 K) Results

3.1. Ground State Reaction Cross-Sections. Reactive cross-sections as a function of translational energy (E_{trans}), for the reactant HBO in its ground vibrational state (0,0,0), were calculated at 10 values of E_{trans} in the 75.31−226.94 kJ mol^{-1} range. By considering this energy range, the channels (iii) leading to H(1)BO + H(2) and (iv and v), both producing HOB + H, can be seen to be closed at the lowest translational energies, becoming open at the highest translational energies. QCT calculations show that at E_{trans} below 154.8 kJ mol^{-1}, only the BO + H_2 products are obtained while the H(1)BO + H(2) appear at about 155 kJ mol^{-1}, with partial cross-sections that increase with translational energy. The enhancement of the reactivity for this channel is so sharp that the reaction cross-section at the highest translational energy considered is higher than that corresponding to the BO + H_2 products. On the other hand, the HOB + H products were not obtained at translational energies below 192 kJ mol^{-1} and the corresponding cross-sections are lower than those for both BO + H_2 and H(1)BO + H(2) product channels in the overall energy range considered. Reaction cross-sections as a function of E_{trans} are shown in Figure 2.

Despite the large error for cross-sections values at their threshold energies, results are included in the figure to show better both the threshold energy for each channel and the sharp increase of the cross-sections with E_{trans} once the corresponding product channel becomes open.

3.2. Energy Disposal in Products. The reactivity of the HBO + H reaction system is rather low, mainly at low translational energies. Hence, the reactant's rotational energy averaged over the reactive trajectories only (E_{rot}) can differ from the $(3/2)k_BT$ value. Consequently, the energy partitioning among the products was studied in terms of the fraction of average accessible energy (E_{acc}) invested in translation, vibration, and rotation of the products ($f_i' = E_i/E_{acc}$). The results of energy disposal concerning the BO + H_2 products are shown in Figure 3 and in Table 1.

As can be seen, f_{trans}' decreases inversely with E_{trans}, while both f_{rot}' and f_{vib}' increase with E_{trans}. The increase of f_{vib}' with E_{trans} comes mainly from the H_2 molecule because the BO vibrational excitation decreases with E_{trans}, while that of the H_2 increases. With regards to the rotational excitation of BO and H_2 molecules, the most important changes in the products rotational excitation as a function of E_{trans} are found for the BO molecule. Thus, it seems that the reactants translational energy reverts mainly in both H_2 vibration and BO rotation. The products' internal energy therefore increases with E_{trans}, and consequently, the product translational energy decreases. This behavior has also been found for the reverse reaction, but some differences were observed. (i) The fraction of available energy that ends up in products translation is higher for the forward HBO + H than for the reverse BO + H_2 reaction. (ii) The fraction of available energy that ends up in products vibration is higher for the reverse reaction, with a triatomic molecule as a product. Moreover, the final products vibrational excitation is much more dependent on E_{trans} for the forward reaction than for the reverse one, where the vibrational energy is nearly unaltered when E_{trans} increases. (iii) The changes in the products rotational excitation are higher for the reverse reaction when E_{trans} increases.

Vibrational and rotational distributions of the products can be seen more easily in Figure 4, where the vibrational distribu-

TABLE 1: BO + H_2 Energy Disposal as a Function of Collision Energy for the H + HBO (0,0,0) Reaction at T_{rot} = 300 K

E_{trans}[a]	f_{trans}'	f_{vib}' (BO)	f_{rot}' (BO)	f_{vib}' (H_2)	f_{rot}' (H_2)	E_{acc}[a]
75.31	0.799 ± 0.074	0.076 ± 0.007	0.020 ± 0.002	0.075 ± 0.006	0.030 ± 0.003	80.95
92.05	0.766 ± 0.033	0.062 ± 0.003	0.030 ± 0.001	0.112 ± 0.005	0.030 ± 0.001	97.69
108.78	0.736 ± 0.024	0.053 ± 0.001	0.042 ± 0.001	0.141 ± 0.003	0.028 ± 0.001	114.43
125.52	0.713 ± 0.013	0.053 ± 0.001	0.055 ± 0.001	0.150 ± 0.003	0.029 ± 0.001	131.16
142.26	0.693 ± 0.011	0.044 ± 0.001	0.070 ± 0.001	0.165 ± 0.003	0.028 ± 0.001	147.9
158.99	0.678 ± 0.011	0.035 ± 0.001	0.085 ± 0.001	0.173 ± 0.003	0.029 ± 0.001	164.64
175.73	0.652 ± 0.011	0.033 ± 0.001	0.097 ± 0.002	0.185 ± 0.003	0.033 ± 0.001	181.37
192.46	0.633 ± 0.012	0.032 ± 0.001	0.108 ± 0.002	0.189 ± 0.003	0.038 ± 0.001	198.11
209.20	0.612 ± 0.012	0.029 ± 0.001	0.109 ± 0.002	0.204 ± 0.004	0.046 ± 0.001	214.84
225.94	0.593 ± 0.013	0.029 ± 0.001	0.112 ± 0.003	0.215 ± 0.005	0.052 ± 0.001	231.58

[a] The units are given in kJ mol^{-1}.

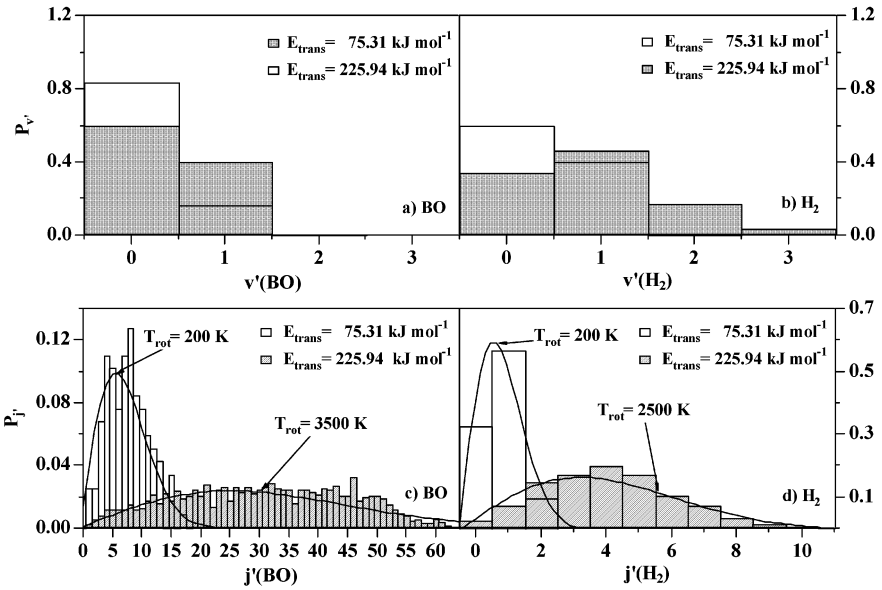

Figure 4. H + HBO (0,0,0) → BO(v,j) + H_2(v,j) reaction at T_{rot} = 300 K. (a) BO vibrational population. (b) H_2 vibrational population. (c) BO (v′ = 0) rotational population. (d) H_2 (v′ = 0) rotational population. In c and d, for comparison with QCT results, the Maxwell Boltzmann rotational distributions are shown (continuous lines).

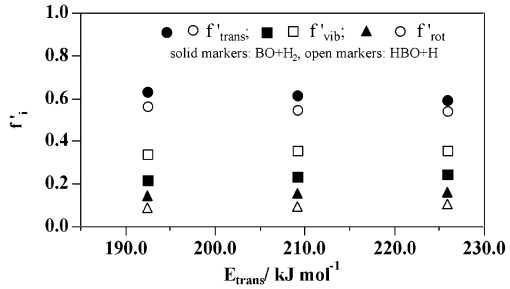

Figure 5. Energy distribution in products at different translational energies (reactant HBO in its ground vibrational state and T_{rot} = 300 K).

tion for BO and H_2 is compared at the lowest and highest E_{trans} values considered. While only two vibrational levels (0 and 1) are populated for the BO molecule, four vibrational levels are populated for H_2. Moreover, at the highest energy studied, the H_2 product shows a vibrational population inversion of the first two levels. Thus, more vibrational energy goes into the newly formed bond. In fact, the vibrational energy average for H_2 clearly increases with E_{trans}; the H_2 vibrational energies are equal to 6.15 and 49.7 kJ mol^{-1}, respectively, at the lowest and highest values of E_{trans} considered. On the other hand, the average BO vibrational energy is small and essentially independent of the translational energy (6.12 and 6.63 kJ mol^{-1} at the lowest and highest values of E_{trans}). Figure 4 also shows the BO and H_2 normalized rotational distributions at two selected translational energies; both are products in their ground vibrational state. As can be seen, the rotational distributions for both products are cold at the lower collision energy considered but very hot at the higher one. This is indicated by the rotational temperature, T_{rot}, fitting QCT-calculated distributions to a Maxwell Boltzmann function.

The title reaction leads to H(1)BO + H(2) and BO + H_2 products at translational energies higher than 158 kJ mol^{-1}. The energy distributions for both products are compared in Figure 5, where only three values are shown because of the high statistical errors (for H(1)BO + H(2) products) at lower energies. The different energy distributions do not change qualitatively when E_{trans} increases. From a quantitative point of view, it can be seen that although the percent of available energy going to internal energy is the same for both product channels, the HBO product has a larger content of vibrational energy than the BO and H_2, while rotational excitation is higher for the diatomic products.

Concerning the HOB + H products channel, only two results are available at the highest values of translational energy considered in the present paper. Our results show that the higher content in both rotational and vibrational excitation corresponds to the HOB angular product. For the HOB + H product channel, about 40% of available energy goes to product translation, while 45 and 15% goes to vibration and rotation, respectively.

3.3. Product Angular Distribution and Reaction Mode. The analysis of the angular distribution reveals that the BO + H_2 products are strongly backscattered in the overall range of translational energies considered. For instance, 100 and 90% of backward scattering were obtained at the lowest and highest values of E_{trans}, respectively. Differential cross-section (DCS) results show angular distributions that become slightly broader when the energy increases and with the maximum of the distribution shifting to lower angles, but in all cases, the products are backward-scattered. This preferential scattering observed for the overall range of translational energies would prove the direct character of those reactive collisions leading to BO + H_2 products, independently of the initial translational energy. This result is in agreement with that found for the reverse reaction, where the direct character of the collision was also observed.[24] Moreover, Figure 1 shows that both minima M1 and M2 are only related to the minimum energy reaction paths connecting reactants with triatomic products and not with the reaction channel leading to BO + H_2 products. In Figure 6, DCSs at several collision energies are given, with the continuous lines corresponding to the best fits obtained from an expansion of Legendre polynomials as explained by Aoiz et al.[42,43]

With regards to the other open reaction channels at higher collision energies, we observed that the percent of backward scattering for the H(1)BO + H(2) products is higher than the forward one (at about 60% independently of the translational energy) but always lower than that corresponding to the BO + H_2 products. The products HOB + H are 36% backward-scattered at 209.2 kJ mol^{-1} of E_{trans}. The percentage of backward

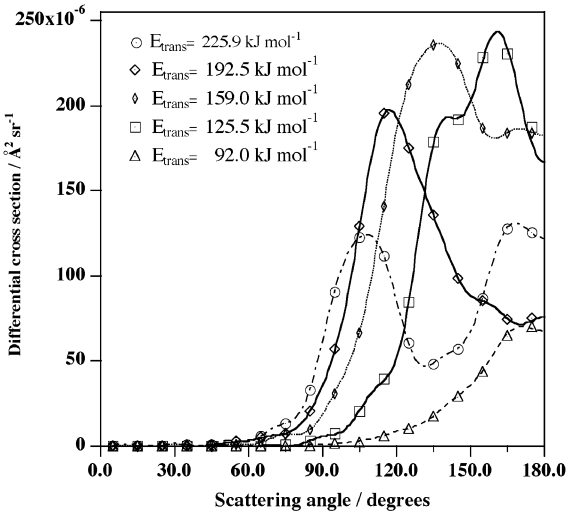

Figure 6. DCSs for BO + H_2 products at several selected translational energies (reactant HBO in its ground vibrational state and T_{rot} = 300 K). The continuous line corresponds to the best fit using an expansion of Legendre polynomials.

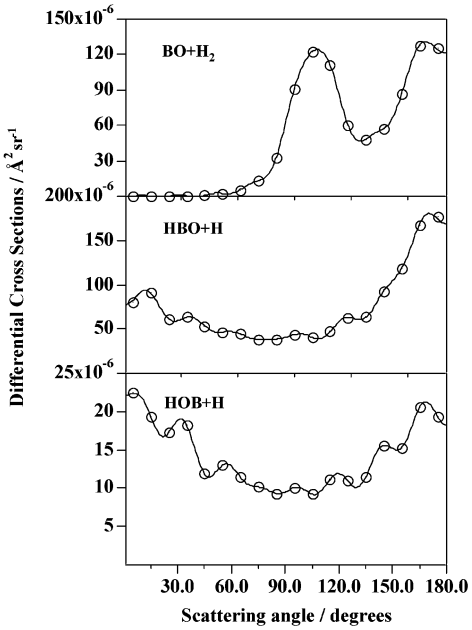

Figure 7. DCSs for the different reaction products at the selected translational energy of 225.9 kJ mol^{-1} (reactant HBO in its ground vibrational state and T_{rot} = 300 K). The continuous line corresponds to the best fit using an expansion of Legendre polynomials.

scattering increases with increasing E_{trans} until it is 50% at 225.94 kJ mol^{-1}. It should be noted that cross-section for the HOB + H channel at 209.2 kJ mol^{-1} was obtained with a statistical error of about 10% while at the energy of 225.94 kJ mol^{-1} the statistical error is about 4%. From a qualitative point of view, angular distributions for both H(1)BO + H(2) and HOB + H products are quite similar, as shown in Figure 7, where the DCSs for the three different reaction channels are given at the highest value of E_{trans} studied.

At the selected energy, both H(1)BO + H(2) and HOB + H reaction products are forward−backward-scattered; the DCS distribution is more symmetrical around 90° for the HOB + H product channel. From this figure, the differences between the H(1)BO + H(2) and the HOB + H product angular distributions and those corresponding to BO + H_2 products are also evident.

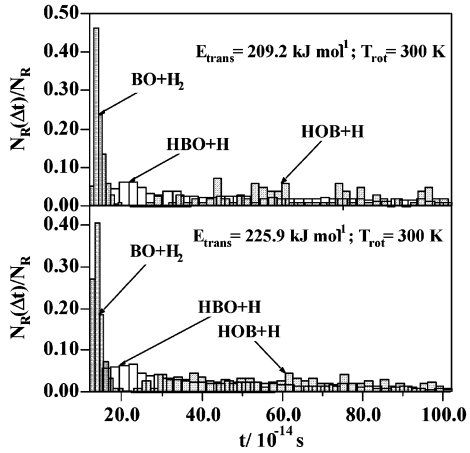

Figure 8. Products collision time distribution at the lowest and highest translational energies investigated (reactant HBO in its ground vibrational state).

More information about the reaction mode can also be obtained from the elapsed time for reactive trajectories, together with the evolution of the interatomic distances and angles during the reactive events. Taking into account that three different product channels can be reached from HBO + H reactants, we should expect the elapsed time distribution for those trajectories exploring some of the minima on the PES to be quite different than the distribution time for those direct trajectories that do not explore such minima. In Figure 8, these time distributions at the two highest translational energies are shown.

The distributions for reactive trajectories leading to H(1)BO + H(2) and HOB + H are seen as very similar, while those for the BO + H_2 products are quite different; they are much more narrow. These differences are also reflected in the value of the average elapsed time. Collision time for the reactive trajectories giving H(1)BO + H(2) and HOB + H is about three and four times larger, respectively, than those for BO + H_2.

In Figure 9a−c, three representative trajectories corresponding to the three different products are shown. These trajectories were selected taking into account their evolution times, which are about the average elapsed time at the selected energy (140, 450, and 590 fs for BO + H_2, H(1)BO + H(2), and HOB + H at 225.94 kJ mol^{-1}, respectively). Figure 9a shows how the H(1)-BO and H(1)OB angles evolve around 180 and 0°, respectively, along the trajectory for approximately 80 fs. Only when the products are clearly separated, when some selected interatomic distances are large enough, do the angles evolve far away from their initial values. This clearly evidences the dominant collinear character for the reaction channel leading to BO + H_2. Consequently, neither M1 nor M2 minima are probed in the reaction pathway. Similar results were obtained by analyzing a large number of trajectories. This confirms both the strong tendency to collinearity of each individual collision and the direct mechanism for the HBO + H → BO + H_2 reaction for which no complex trajectories were found. These results are in good agreement with the previous ones obtained for the reverse reaction.[24]

The evolutions of the angles are very different when compared with those shown in Figure 9b,c for reactive trajectories producing H(1)BO + H(2) and HOB + H. Reactive trajectories leading to H(1)BO + H(2) and HOB + H products show a very similar pattern; both are complex trajectories that contrast with the direct character found when BO + H_2 products are obtained.

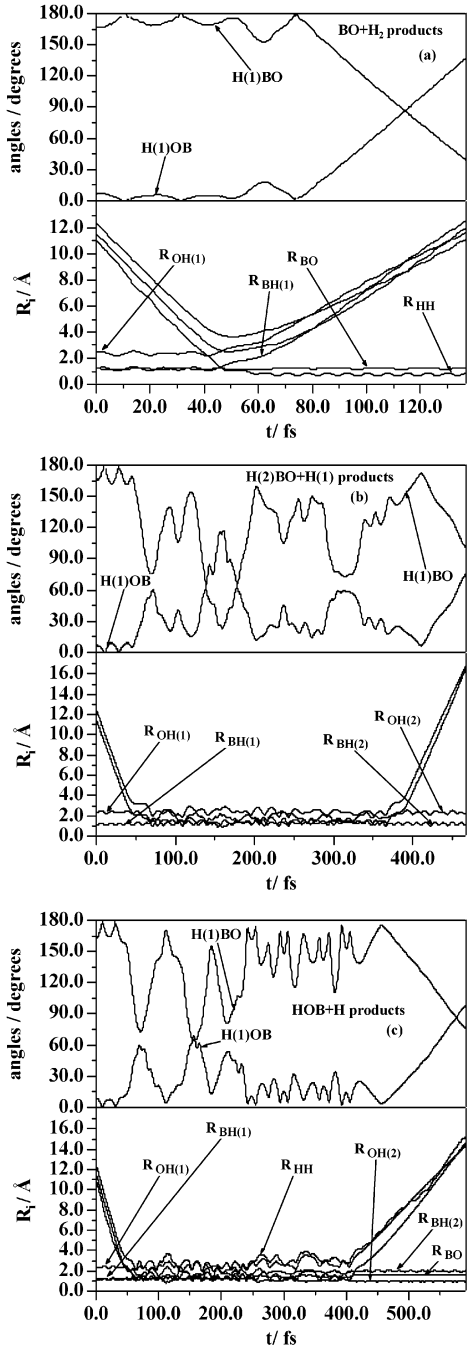

Figure 9. Time evolution of the internuclear distances and angles for selected reactive trajectories leading to (a) BO + H_2, (b) H(1)BO + H(2), and (c) HOB + H.

4. Reactant Vibrational Excitation: The H + HBO (v_{BO},v_2,v_{BH}) Results

4.1. Influence of the Vibrational Excitation on the Reaction Cross-Sections: The (v_{BO},0,0), (0,0,v_{BH}), and (0,v_2,0) States. To assess the vibrational energy, selectivity on the reactivity of all HBO vibrational modes (BO and BH stretching and degenerate bending, here represented as v_{BO},v_{BH}, and v_2, respectively) was excited. As a first step, more than 20 vibrational states were considered; most calculations were performed at 75.31 kJ mol^{-1} of translational energy and at the rotational temperature of 300 K. Some calculations at higher energies were also carried out so as to better analyze the effect of vibrational excitation on the reactivity of product channels other than BO + H_2. Reactive cross-sections obtained by exciting the different vibrational modes were compared among each other and also compared with those modes corresponding to the ground vibrational state of the reactant molecule. Results reported here and in the preceding section will also be compared in terms of the total energy (E_{total}).

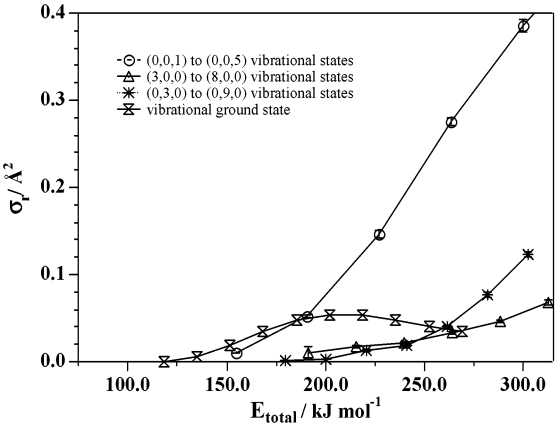

Figure 10. Reaction cross-sections as a function of total energy at different HBO initial vibrational states and 300 K of rotational temperature.

As a general trend, we observed that reactive cross-sections for both H(1)BO + H(2) and HOB + H reaction products are inappreciable and are essentially unaffected by the vibrational excitation of the reactant molecule. Although H(1)BO + H(2) and HOB + H product channels are energetically accessible at most of the vibrational initial conditions considered, we found a probability approaching zero for the formation of triatomic products. For instance, at E_{total} = 299.6 kJ mol^{-1} with E_{trans} = 75.31 kJ mol^{-1}, T_{rot} = 300 K, and the HBO molecule in the (0,0,5) initial vibrational level, which is the maximum vibrational excitation of the BH stretching mode considered in this study, over a total of 500 000 trajectories, 3025 led to BO + H_2, while only two yielded HBO + H and three yielded HOB + H. Thus, it is clear that the BH stretching excitation does not enhance the formation of triatomic products. A similar behavior has been obtained with BO stretching excitation.

Taking the previous considerations into account leads one to expect that vibrational excitation in the bending mode (v_2) could be most effective in promoting the formation of H(1)BO + H(2) and HOB + H products. However, when a bending vibrational excitation is performed, only a very small number of reactive trajectories leading to triatomic reaction products is found. For instance, at E_{total} = 302.1 kJ mol^{-1} with E_{trans} = 75.31 kJ mol^{-1}, T_{rot} = 300 K, and the HBO molecule in the (0,9,0) initial vibrational level, which is the maximum vibrational excitation of the bending mode considered in this study, over a total of 500 000 trajectories, 1282 produce BO + H_2, while only 16 lead to HBO + H and seven lead to HOB + H products. Consequently, we can conclude that vibrational excitation does not facilitate the formation of triatomic products.

Concerning the BO + H_2 reaction products, the BH stretching excitation in the HBO reactant was found to cause a high enhancement of the reactivity. Results also show that vibrational excitation of BO stretching or that of degenerate bending, at moderate collision energies, is less effective in promoting the reactivity than is E_{trans}. At the highest values of E_{total}, bending excitation is more effective in promoting reactivity than the BO stretching excitation is. All of these results are shown in Figure 10, where the cross-sections for the formation of the BO + H_2 products are reported as a function of total energy.

The previous study on the reaction channel leading to BO + H_2 products, performed at 75.31 kJ mol^{-1} of translational

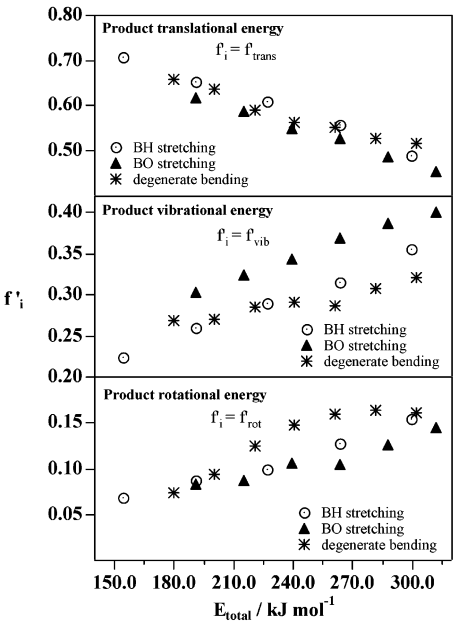

Figure 11. BO + H_2 product energy disposal (in terms of the fraction of accessible energy) as a function of HBO initial vibrational energy (E_{trans}= 74.31 kJ mol^{-1} and T_{rot} = 300 K).

energy, was completed using results obtained at other translational energies and also considering other vibrational states with two excited vibrational modes. The results for some of these states have proved the effectiveness of BH stretching enhancing reactivity by comparing sets of results with the same total energy.

The same qualitative results were obtained for the isoelectronic H + HCN reaction.[21] For both reactions (HBO + H and HCN + H) and at the same translational energy, the (3,0,2) vibrational state produces an enhancement in reactivity with respect to the (0,0,2) state. The enhancement is not, however, as great as for the (0,0,4) state. As explained in regard to HCN + H reactions,[21] these results for HBO + H suggest that the BO mode is not as strongly coupled with motions leading to reaction as the BH stretch. This has been explained in terms of the vibrational modes at the transition state.[24]

4.2. Influence of the Reactant Vibrational Excitation on the Products Energy Disposal. The energy partitioning among products as a function of total energy for different (0,0,v_{BH}), (v_{BO},0,0), and (0,v_2,0) initial vibrational states at 74.31 kJ mol^{-1} of translational energy and 300 K of rotational temperature was also investigated. As far as the dependence on vibrational energy is concerned, as a general trend for the predominant reaction channel, most of the available energy was found to be channeled into the translation and vibration of the products. Results of the energy partitioning are given in Figure 11. In the upper panel of the figure, it can be seen that the percent of available energy going into translation decreases as E_{total} increases. On the other hand, the percentage that corresponds to both vibration and rotation of the products increases (see medium and lower panels of Figure 11). These results are not unlike those found by analyzing products energy disposal as a function of translational energy; the HBO is in its ground (0,0,0) vibrational state (Section 3.2).

On the other hand, Figure 11 shows that the amount of translational energy going into the products seems to depend only on total energy (top panel), while vibrational and rotational contents depend on the excited vibrational state (medium and bottom panels). Looking at the medium panel, we also see that the BO bond stretching more efficiently channels the vibrational energy into the products than do the remaining vibrational modes. The lower panel of Figure 11 shows the higher rotational content of the products obtained when the bending mode is excited, while both BH and BO bond stretching channel about the same fraction of available energy into rotation of the products.

Considering BO and H_2 products separately, it has been observed that (i) the fraction of accessible energy going into vibrational excitation of the products is higher for the H_2 molecule than for the BO molecule (f_{vib}' (H_2) > f_{vib}' (BO)), independently of which normal vibrational mode is excited; (ii) BH or BO stretching excitation of the HBO reactant molecule gives H_2 products with the same content of vibrational energy (in terms of f_{vib}'); and (iii) when a specific vibrational mode is excited, the energy increase reverts mainly in H_2 vibrational excitation while the vibrational content of the BO product remains nearly unaffected (the higher vibrational excitation for BO product is obtained from the BO stretching excitation).

4.3. Angular Distribution and Reaction Mode at Several Vibrational Initial Conditions. In Section 3.3, the BO + H_2 products were seen as being predominantly backward-scattered irrespective of collision energy. On the contrary, the H(1)BO + H(2) and HOB + H products show a forward/backward scattering. As H(1)BO + H(2) and HOB + H products are scarce, only the BO + H_2 angular dependence on the reactant vibrational state can be properly analyzed. At any initial vibrational condition, the BO + H_2 products show the same direct character observed for the ground state when the translational energy was changed. This is reflected by the average elapsed time value for reactive trajectories, which is always less than 200 fs. For any initial vibrational state, more than 90% of reactive trajectories are backward-scattered.

When the scarce products H(1)BO + H(2) are also formed (no representative results for HOB + H products have been obtained), the angular distribution pattern shows a nearly symmetric forward−backward angular distribution and the average elapsed time is about 500 fs.

5. Reactant Rotational Excitation: The H + HBO (0,0,0, T_{rot}) Results

5.1. Influence of the Rotational Temperature in the Cross-Sections. The different values of the rotational temperatures, ranging between 300 and 3000 K, comprise our last step in the study of the influence of the different energies on the HBO + H reaction.

Most of the QCT calculations were performed at 175.73 kJ mol^{-1} of translational energy, with the HBO molecule in its vibrational ground state. To analyze whether changes in rotational energy influence the formation of HBO + H and HOB + H, calculations at 3000 K were also carried out at the three highest values of E_{trans} considered in the present study (192.46, 209.20, and 225.94 kJ mol^{-1}). Acceptable statistical results are found by running batches of 500 000 trajectories, except when triatomic products are formed, in which case batches of 1 500 000 trajectories are required.

The results at E_{trans} = 175.73 kJ mol^{-1} show that cross-sections for the HBO + H → BO + H_2 reaction channel are almost unchanged by an increase in the rotational temperature from 300 to 3000 K (see Figure 12). In Section 3.1, where the dependence of the reactivity as a function of E_{trans} was investigated, larger changes in the cross-sections were observed for the same range of total energy.

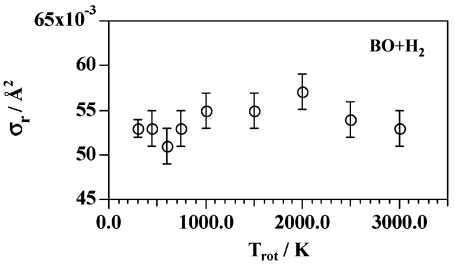

Figure 12. Reaction cross-section leading to BO + H_2 products as a function of rotational temperature (reactant HBO in its ground vibrational state, E_{trans} = 175.73 kJ mol^{-1}).

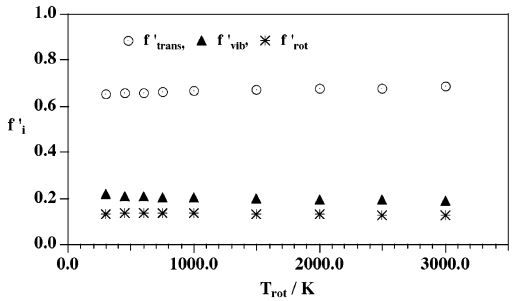

Figure 13. Product energy disposal (in terms of the fraction of accessible energy) as a function of total energy at different rotational temperatures (reactant HBO in its ground vibrational state, E_{trans} = 175.73 kJ mol^{-1}).

When results for the HBO + H → BO + H_2 reaction are compared with those for the BO + H_2 → HBO + H reverse reaction, these reactions are seen to show a dependence of the cross-sections on rotational energy quite different one from the other. For the reverse BO + H_2 reaction, reactant rotational excitation produces an inhibition of the reactivity; the observed cross-section decrease is irrespective of which reactant molecule is rotationally excited. This behavior was explained by taking into account the fact that an increase in the rotational quantum number results in greater difficulties in allowing the system to collide with the proper, i.e., collinear, orientation.[24]

To understand the different dependence on rotational energy observed for forward HBO + H and reverse BO + H_2 reactions, the particular reactant rotational excitation was considered. In the study of the BO + H_2 → HBO + H reaction,[24] QCT calculations were performed for several values of the rotational quantum number of the diatomic molecules (BO, $0 \le j \le 20$, and H_2, $0 \le j \le 4$), being the corresponding rotational energies in the energy ranges 0−9.3 and 0−14.8 kJ mol^{-1} for BO and H_2 molecules, respectively. For the HBO + H reaction, changing T_{rot} from 300 to 3000 K increases the rotational energy by about 20 kJ mol^{-1}.

To explain the different behavior of the reactions as a function of the reactant rotational excitation, an estimation of the BO, H_2, and HBO rotational periods was made and compared with the half collision time for reactive trajectories. The results show that for the H + HBO reaction in the overall range of rotational initial conditions, the HBO rotational period is always larger than the half collision time, while for the BO + H_2 reverse reaction the rotational period of both H_2 and BO is lower than the half collision time.

Reactive cross-sections for the different product channels for the HBO + H reaction calculated at 300 and 3000 K at the highest values of E_{trans} are given in Table 2, where it can be seen that little dependence on rotational energy was found for the cross-sections related with the formation of BO + H_2 products at the energies considered. Table 2 also shows the important enhancement of the reactivity for the HBO + H and HOB + H product channels when rotational energy increases, except at the highest translational energy.

5.2. Influence of the Reactant Rotational Excitation on the Products Energy Disposal. The increase of reactant rotational energy causes minor changes in the energy distribution of the products. However, the trend followed for the different products is the opposite of that found when the translational reactant energy increased. Results show that almost all of the increase of rotational energy reverts to a translation of products (E_{trans}'), i.e., for E_{trans} = 175.73 kJ mol^{-1}, E_{trans}' = 118.2 kJ mol^{-1} at 300 K and E_{trans}' = 140.7 kJ mol^{-1} at 3000 K; f_{trans}' is 0.65 and 0.68, respectively. However, a diminution was observed by increasing E_{trans} (considering the same interval of total energy). Within the statistical error, the product's rotational content remains unmodified when reactant rotational energy is increased. Consequently, f_{vib}' decreases by the same amount as the corresponding increases in f_{trans}'. The general trends of the products energy distribution can be seen in Figure 13, where results for BO + H_2 products are shown.

By comparing those results obtained at 300 K and at 3000 K at different translational energies, similar trends for BO + H_2 products were found. This is like the behavior found for the BO + H_2 reverse reaction, where the effect of rotational energy in product energy disposal was seen to be very small. Nevertheless, for the reverse reaction, the percent of accessible energy going to products translation is less than for the direct reaction. This energy is about 1.5% when the rotational state of the BO molecule moves from j = 0 to j = 20 (without rotational excitation of H_2 molecule). Moreover, no change was observed without rotational excitation of the BO molecule when H_2 was rotationally excited. In fact, in this latter case, the increase of accessible energy was distributed mainly as vibrational energy of the products.

When products other than BO + H_2 are formed, the increase of reactant rotational energy is observed to give HBO + H and HOB + H products with a lower content of translational energy and a higher internal energy. By comparing results obtained at 300 and 3000 K at several translational energies, we found that the increase of rotational energy reverts mainly into vibration and rotation. As a consequence, the percent of accessible energy going to products translation diminishes while the corresponding for vibration and rotation increase.

5.3. Angular Distribution and Reaction Mode at Several Rotational Temperatures. As it was shown in Section 3.3 under different initial conditions, the BO + H_2 products are preferentially backward-scattered, but some changes in the

TABLE 2: Reaction Cross-Sections at Several Translational Energies (at 300 and 3000 K)

E_{trans} (kJ mol^{-1})	175.73	192.46	209.20	225.94
σ_r(BO + H_2, 300 K) (Å^2)	0.0532 ± 0.0009	0.0472 ± 0.0009	0.0406 ± 0.0008	0.0352 ± 0.0008
σ_r(BO + H_2, 3000 K) (Å^2)	0.0530 ± 0.0009	0.0490 ± 0.0009	0.0420 ± 0.0009	0.037 ± 0.001
σ_r(HBO + H, 300 K) (Å^2)	0.0007 ± 0.0001	0.0036 ± 0.0002	0.0155 ± 0.0005	0.0421 ± 0.0009
σ_r(HBO + H, 3000 K) (Å^2)	0.0018 ± 0.0002	0.0068 ± 0.0004	0.0234 ± 0.0008	0.049 ± 0.001
σ_r(HOB + H, 300 K) (Å^2)			0.0016 ± 0.0002	0.0088 ± 0.0004
σ_r(HOB + H, 3000 K) (Å^2)		0.0021 ± 0.0002	0.0074 ± 0.0004	0.0191 ± 0.0007

angular distribution were observed by increasing reactant rotational energy: the percent of backward scattering changes from 97.2% at 300 K to 83.2% at 3000 K. This change in the products angular distribution is the highest one observed by modifying initial energy conditions. In fact, in the same interval of total energy as that considered here, hardly any changes in products angular distribution were found when the HBO reactant was vibrationally excited. No changes are observed with the vibrational excitation of the bending mode (backward scattering about 99%) and minor changes (backward scattering between 99 and 97%) by increasing the vibrational excitation of both stretching modes.

Concerning the angular distribution for the H(1)BO + H(2) and HOB + H reaction products, no important changes were observed by increasing the temperature from 300 to 3000 K. For both products, a very similar forward/backward ratio is found at the same translational energy when the rotational temperature changes from 300 to 3000 K; both products show a nearly symmetric forward−backward angular distribution. Moreover, the elapsed time average for the reactive trajectories for both reaction channels is the same irrespectively of the rotational temperature considered.

6. Discussion

The reaction cross-section as a function of E_{trans} for the different product channels, with the reactant HBO in its ground vibrational state, reflects the topology of the PES. Moreover, ground state reactive cross-sections leading to BO + H_2 are similar in magnitude to those found for other endoergic reactions such as H + HCN[21] and H + H_2O.[41] The higher reactivity for the diatom−diatom BO + H_2 reaction[24] than for the atom−triatom HBO + H reaction was also observed for HCN + H and CN + H_2 reactions.[21]

Moreover, the HCN + H reaction[21] qualitatively shows the same vibrational distribution into products as the title reaction, with a higher content in the H_2 fragment rather than in the CN one. Moreover, a higher content into CN vibration was obtained when the CN stretching bond was excited. As pointed out by Kreher et al.,[20] the vibrational excitation of the CN molecule seems to be a consequence of the initial vibration of HCN.

Taking the excitation of both vibrational stretching modes all together, we also proved the effectiveness of BH stretching excitation enhancing reactivity. For instance, by comparing the results obtained for two pairs of initial vibrational states, where each partner has a nearly identical available energy (in particular for the two couples ((4,0,2)−(1,0,4) and (5,0,2)−(2,0,4)), we observed that the vibrational content in the BO product molecule for initial states (4,0,2) and (5,0,2) is higher than those obtained from the (1,0,4) and the (2,0,4) states, respectively. These results also show the same qualitative behavior as the experimental[20] and theoretical[21] results obtained for the HCN + H reaction.

The main difference between HCN + H and HBO + H reactions deals with the energy dependence at the highest collision energies, when other products than BO + H_2 appear. When this is the case, the BO + H_2 cross-sections show a noticeable decrease. This diminution can be explained in terms of the competition between all of the product channels that are involved in the HBO + H reaction.

Regarding the energy disposal in BO + H_2 products, the fact that a significant portion of the accessible energy goes to H_2 vibrational energy, while little vibration goes to the BO bond, taken together with the increase of the H_2 vibrational content with E_{trans}, indicate that the H_2 stretch mode is coupled to the reaction coordinate. However, the results seem to indicate that the BO bond stretch is uncoupled. The higher content of vibrational energy for the H(1)BO + H(2) or HOB + H products, as compared with the BO + H_2 products, is mainly due to the increase in the number of the normal vibrational modes. For these triatomic products, the BO stretching is also the less vibrationally excited mode, while higher excitation is observed for both BH stretching and BH bending modes. This, it will be recalled, was seen from the analysis (for a great number of reactive trajectories) of the interatomic distances evolution when products are already formed. All of these results suggest that the BO bond behaves like a spectator.

Results regarding the product angular distribution as a function of E_{trans} reflect the difference between the reaction mode leading to BO + H_2 products and that leading to triatomic products. BO + H_2 products are strongly backward-scattered, while the remaining products show a nearly symmetric forward−backward angular distribution; these behaviors are almost independent of the initial energy conditions. These results suggest a direct rebound mechanism for collisions leading to BO + H_2, while a nondirect or complex mechanism is related to both triatomic products. A preferential scattering for direct reactions is known to indicate that the reaction process must be over before the colliding pair of reactants has time to execute one or more rotations about each other. On the other hand, the no preferential scattering found for HBO + H and HOB + H products might be an indication that the colliding pair remains together for a long time, the collision thus occurring in a complex way. These results indicate that the characteristics of the PES areas explored by the trajectories producing BO + H_2 or triatomic products are very different, with reactive trajectories leading to H(1)BO + H(2) or HOB + H exploring the M1 and/or M2 zones on the PES.

The evolution of the internuclear distances and angles along the collision route allows corroboration of the direct and complex reaction mode for BO + H_2 and triatomic products, respectively. The evolution of the distances and angles for those trajectories producing HBO + H or HOB + H, unlike the observations for BO + H_2 products, is snarled, however. They indicate the formation of a quasibound, long-lived complex, with a long enough lifetime to allow energy exchange between the different vibrational modes, thus losing any information about the trajectory initial conditions. In fact, the slight forward−backward asymmetry observed for HBO + H products suggests that an osculating collision complex (with its lifetime being somewhat shorter than the corresponding rotational period) is formed,[44,45] as can be concluded by comparing the rotational period with the estimated complex lifetime obtained from the average elapsed time for reactive trajectories leading to HBO + H. The same behavior can be attributed to the formation of HOB + H products; however, the poor statistics add a good deal of uncertainty to the results obtained.

The inefficacy of the HBO reactant vibrational excitation in promoting the formation of triatomic products to overcome the potential barriers connecting reactants with M1 or M2 minima, even when the total energy is large enough, can be justified in terms of the location of the potential energy barriers (TS2 and TS4) on the PES. Results suggest that the PES does not efficiently mix vibrational and translational energies, being unable to pump vibrational into translational energy, as required according to the earlier character of the TS2 barrier. As a consequence, only the reaction channel leading to diatomic BO + H_2 fragments (reached after surmounting a late barrier (TS1)) is effectively open to reaction. Among all of the HBO reactant vibrational normal modes, less efficiency in promoting reactivity of the H(1)BO + H(2) or HOB + H product channels was found

for the BH and BO bond-stretching excitation. This result is not surprising given that both stretching modes tend to preserve the collinearity of the triatomic reactant.

Concerning BO + H_2 products, the most effective enhancement of reactivity from vibrational excitation of the BH bond stretching can be justified in terms of the vibrational modes at the TS1 transition state, as was done in ref 24. In the present case, the average enlargement of the BH bond that must be broken to obtain the BO + H_2 products reinforces the justification.

The main results regarding the energy disposal into the products as a function of vibrational excitation of the reactants can be explained by taking into account the newly formed bond and the broken bond. From this point of view, the vibrational energy located in the BH bond at the beginning of the collision can be seen as having to be transferred to other energies. On the other hand, that energy located in the BO bond at the beginning of the trajectory can remain in it. Similarly, from the same analysis previously carried out at the transition state, the higher content on product rotational energy obtained from bending, better than from stretching vibrational excitation, can be explained by taking into account that TS1 normal modes correlating asymptotically with the reactant bending mode are those degenerate of Π symmetry (see refs 24 and 25). These modes actually correspond to hindered rotations in the transition state and are the ones responsible for transferring reactant vibrational bending energy to product rotational energy. Furthermore, the fact that both BH and BO stretching vibrations channel the same amount of products rotational energy can also be explained by the same correlation arguments. The higher content on product vibrational energy when the vibrational excitation comes from BO bond stretching instead of BH bond stretching can be interpreted in terms of the essentially spectator character of the BO bond. This bond remains practically unaltered throughout the collision process, while the BH bond must be broken in order to lead to the BO + H_2 products. Vibrational energy initially in the BH bond needs to be redistributed when products are formed. Vibrational energy initially in the BO bond does not need to be redistributed and shows a strong adiabatic character.

Comparison between the reactants rotational period and the half collision time for reactive trajectories in forward HBO + H and reverse BO + H_2 reactions allows us to explain the different trends of these reactions as a function of rotational energy. As the rotational period for HBO reactant is always larger than the half collision time, little change in the initial orientation of the reactants in the HBO + H reaction takes place along the semicollision before reaction. However, as the rotational period of both BO and H_2 reactants is lower than the half collision time, the collinear preferred orientation of the reactants is disrupted and, consequently, a diminution of the reactant cross-sections is found for the case of the BO + H_2 reaction when the rotational energy is increased.

For the title reaction, the null dependence on rotational energy to produce BO + H_2 contrasts with the high enhancement of the reactivity to form triatomic products, mainly at low and moderate rotational temperatures. The different behavior can be explained from the different parts of the PES explored by reactive trajectories that produce diatomic or triatomic products, because it is clear that the cross-section as a function of rotational energy is sensitive to the changes in PES.[46,47] On the other hand, by increasing the rotational temperature, the average elapsed time for reactive trajectories (and thus the collision time) leading to triatomic products increases. The rotational excitation then becomes less favorable than at low and moderate rotational temperatures. Concerning BO + H_2 products, the impossibility of exploring the M1 or M2 minima on the PES when these products are obtained excludes the possibility of a change in the reaction mechanism induced by rotational excitation. In this case, taking into account that the average collision time for reactive trajectories does not change increasing rotational energy, the diminution of the BO + H_2 backward scattering can be interpreted in terms of the enlargement of the range of impact parameters that contribute to the reactive events. In fact, the range of impact parameters contributing to reactive events leading to BO + H_2 products becomes larger by increasing rotational energy than by increasing translational energy.

Acknowledgment. This work has been supported by the Spanish DGICYT (Projects PB97-0919 and BQU2001-3018) and the Generalitat de Catalunya (CUR 20001SGR-00041). Thanks are also due to the Centre de Supercomputació de Catalunya (CESCA) for the computational facilities used in carrying out part of the present calculations.

References and Notes

(1) *Phys. Chem. Chem. Phys.* Special Issue Chemical Reaction Theory, **1999**, *1*.
(2) *Phys. Chem. Chem. Phys.* Special Issue, **2000**, *2*.
(3) Bowman, J. M.; Wang, D. *Advances in Molecular Vibrations and Collision Dynamics*; Bowman, J. M., Ed.; JAI Press: Greenwich, CT, 1994; Vol. 2B, p 187.
(4) (a) Metz, R. B.; Thoemke, J. D.; Pfeiffer, J. M.; Crim, F. F. *J. Chem. Phys.* **1993**, *99*, 1744. (b) Pfeiffer, J. M.; Metz, R. B.; Thoemke, J. D.; Woods, E., III; Crim, F. F. *J. Chem. Phys.* **1996**, *104*, 4490. (c) Kreher, C.; Theinl, R.; Gericke, K. H. *J. Chem. Phys.* **1996**, *104*, 4481.
(5) Zare, R. N. *Nature* **1993**, *365*, 105.
(6) Alagia, M.; Balucani, N.; Casavecchia, P.; Stranges, D.; Volpi, G. G. *J. Chem. Soc., Faraday Trans.* **1995**, *91*, 575.
(7) Metz, R. B.; Pfeiffer, J. M.; Thoemke, J. D.; Crim, F. F. *Chem. Phys. Lett.* **1994**, *221*, 347.
(8) Szichman, H.; Varandas, A. J. C. *J. Phys. Chem. A* **1999**, *103*, 1967 and references therein.
(9) Ochoa de Aspuru, G.; Clary, D. C. *J. Phys. Chem. A* **1998**, *102*, 9631.
(10) Szichman, H.; Baer, M.; Volpp, H. R.; Wolfrum, J. *J. Chem. Phys.* **1999**, *111*, 567.
(11) Rougeau, N.; Kubach, C. *Chem. Phys. Lett.* **1999**, *299*, 120.
(12) Kosmas, A. M.; Drougas, E. *Chem. Phys.* **1998**, *229*, 233.
(13) Che, D.-C.; Liu, K. *Chem. Phys. Lett.* **1995**, *243*, 290 and references therein.
(14) Che, D.-C.; Liu, K. *Chem. Phys.* **1996**, *207*, 367.
(15) Wang, J.-H.; Liu, K.; Schatz, G. C.; ter Horst, M. *J. Chem. Phys.* **1997**, *107*, 7869.
(16) Takayanagi, T.; Schatz, G. C. *Chem. Phys. Lett.* **1997**, *265*, 410.
(17) Takayanagi, T.; Schatz, G. C. *J. Chem. Phys.* **1997**, *106*, 3227.
(18) Bethardy, G. A.; Wagner, A. F.; Schatz, G. C.; ter Horst, M. A. *J. Chem. Phys.* **1997**, *106*, 6001.
(19) Zhu, W.; Zhang, J. Z. H.; Zhang, Y. C.; Zhang, Y. B.; Zhan, L. X.; Zhang, S. L.; Zhang, D. H. *J. Chem. Phys.* **1998**, *108*, 3509.
(20) Kreher, C.; Rinnenthal, J. L.; Gericke, K. H. *J. Chem. Phys.* **1998**, *108*, 3154.
(21) Troya, D.; Baños, I.; González, M.; Wu, G.; ter Horst, M. A.; Schatz, G. C. *J. Chem. Phys.* **2000**, *113*, 6253 and references therein.
(22) Page, M. *J. Phys. Chem.* **1989**, *93*, 3639.
(23) Garland, N. L.; Stanton, C. T.; Nelson, H. H.; Page, M. *J. Chem. Phys.* **1991**, *95*, 2511.
(24) Sogas, J.; Albertí, M.; Giménez, X.; Sayós, R.; Aguilar, A. *J. Phys. Chem. A* **1997**, *101*, 8877.
(25) Sogas, J.; Albertí, M.; Giménez, X.; Aguilar, A. *Chem. Phys. Lett.* **2001**, *347*, 451.
(26) Szichman, H.; Gilibert, M.; Albertí, M.; Giménez, X.; Aguilar, A. *Chem. Phys. Lett.* **2002**, *353*, 446.
(27) Albertí, M.; Sayós, R.; Solé, A.; Aguilar, A. *J. Chem. Soc., Faraday Trans.* **1991**, *87*, 1057 and references therein.
(28) Raz, T.; Levine, R. D. *Chem. Phys. Lett.* **1994**, *226*, 47.
(29) Aoiz, F. J.; Bañares, L.; D'mello, M. J.; Herrero, V. J.; Rábanos, V. S.; Schneider, L.; Wyatt, R. E. *J. Chem. Phys.* **1994**, *101*, 5781.
(30) Aoiz, J.; Bañares, L.; Díez-Rojo, T.; Herrero, V. J.; Rábanos, V. S. *J. Phys. Chem.* **1996**, *100*, 4071.

(31) Raz, T.; Levine, R. D. *J. Phys. Chem.* **1995**, *99*, 7435.
(32) Raz, T.; Levine, R. D. *J. Phys. Chem.* **1995**, *99*, 13713.
(33) Ceballos, A.; García, E.; Rodríguez, A.; Laganà, A. *Chem. Phys. Lett.* **1999**, *305*, 276.
(34) Ceballos, A.; García, E.; Rodríguez, A.; Laganà, A. *J. Phys. Chem. A* **2001**, *105*, 1797.
(35) Troya, D.; Lendvay, G.; González, M.; Schatz, G. C. *Chem. Phys. Lett.* **2001**, *343*, 420.
(36) Troya, D.; González, M.; Schatz, G. C. *J. Chem. Phys.* **2001**, *114*, 8397.
(37) Murrell, J. N.; Carter, S.; Farantos, S. C.; Huxley, P.; Varandas, A. J. C. *Molecular Potential Energy Functions*; John Wiley & Sons: New York, 1984.
(38) Sayós, R. Ph.D. Thesis, Universitat de Barcelona, 1989.
(39) Hase, W. L. *QCPE Bull.* **1983**, 453.
(40) Porter, R. N.; Raff, L. M. *Dynamics of Molecular Collisions*; Miller, W. H., Ed.; Plenum Press: New York, 1976; Part B.
(41) Bradley, K. S.; Schatz, G. C. *J. Chem. Phys.* **1998**, *108*, 7994.
(42) Aoiz, F. J.; Herrero, V. J.; Sáez Rábanos, V. *J. Chem. Phys.* **1992**, *97*, 7423 and references therein.
(43) Aoiz, F. J.; Bañares, L.; Herrero, V. J. *J. Chem. Soc., Faraday Trans.* **1998**, *94*, 2484.
(44) *Molecular Reaction Dynamics and Chemical Reactivity*; Levine, R. D., Bernstein, R. B., Eds.; Oxford University Press: Oxford, 1987.
(45) Albertí, M.; Solé, A.; Aguilar, A. *J. Chem. Soc., Faraday Trans.* **1991**, *87*, 37.
(46) Sathyamurthy, N. *Chem. Rev.* **1983**, *83*, 601.
(47) Albertí, M.; Prieto, M.; Aguilar, A. *J. Chem. Soc., Faraday Trans.* **1992**, *88*, 1615.